

Low-Rank Methods in Event Detection

Jakub Mareček*, Stathis Maroulis*,
Vana Kalogeraki, Dimitrios Gunopulos

August 1, 2022

Abstract

We present low-rank methods for event detection. We assume that normal observations come from a low-rank subspace, prior to being corrupted by a uniformly distributed noise. Correspondingly, we aim at recovering a representation of the subspace, and perform event detection by running point-to-subspace distance queries in ℓ^∞ , for each incoming observation. In particular, we use a variant of matrix completion under interval uncertainty on a suitable flattening $M \in \mathbb{R}^{m \times n}$ of the input data to obtain a low-rank model $M \approx L \times R$, $L \in \mathbb{R}^{m \times r}$, $R \in \mathbb{R}^{r \times n}$, $r \ll m$. On-line, we compute the distance of each incoming $x \in \mathbb{R}^n$ to the space spanned by R . For the distance computation, we present a constant-time algorithm with a one-sided error bounded by a function of the number of coordinates employed. Our experimental evaluation illustrates the benefit of the approach proposed.

1 Introduction

With the rise of Smart Cities and the Internet of Things more generally, many cities have been instrumented with a large number of sensors capable of capturing important statistics, such as volumes of traffic and average speeds of cars passing through urban intersections. Although the information from each of the sensors can be useful in isolation (*e.g.*, maintaining statistics about traffic, pollution, bus speeds, etc.), the combination of the information across multiple sensor types could provide more value. However, processing heterogeneous sensors data poses several challenges. One of the main challenges is dealing with the velocity and, when accumulated, volume of the data. A city can have thousands of sensors sampling at kHz rates. For example, in a network of 10,000 sensors, sampling with 1 byte resolution at 1 kHz, one obtains close to 311 TB of data per year that needs to be analyzed to estimate what is normal. The second challenge

*J.M. is with IBM Research and can be reached at jakub.marecek@ie.ibm.com; S.M. and V. K. are with the Athens Univ. of Economics and Business; D.G. is with the Univ. of Athens. The work received funding from the European Union Horizon 2020 Programme (Horizon2020/2014-2020), under grant agreement no. 688380.

involves detecting an event in real-time. An automated event detection is useful in cases that the event is detected within seconds after it occurs, such as when a road is completely blocked, before people start venting their frustration on social media or dialing their phones. Another common challenge are missing values and failures of sensors. It is very common for sensors to stop working or start reporting wrong values (*e.g.*, negative car flow). Finally, there is measurement noise.

To overcome these challenges, we propose novel low-rank methods for event detection. Throughout, we consider uniformly distributed noise, but let us present the model first in the noise-free case. There, events correspond to points lying outside a certain subspace. To estimate the sub-space, we flatten the input data to a matrix and apply state-of-the-art low-rank matrix-factorization techniques. In particular, we factorize the original matrix into two smaller matrices, whose product approximates the original matrix. Subsequently, we develop a point-in-subspace membership test capable of detecting whether new samples are within the subspace spanned by the columns of one of the factors (smaller matrices). An affirmative answer is interpreted as an indication that the samples from the sensors present normal behaviour. In the case of a negative answer, a point-to-subspace distance query can estimate the extent of abnormality of an event. To our knowledge, this is the first application of these techniques in event detection.

Our contributions are:

- a general framework for representing what is an event and what is a non-event, considering *heterogeneous data*, which are possibly *not sampled uniformly*, with *missing values* and *measurement errors*, based on matrix factorization,
- A novel randomized event detection technique, implemented via a *point-to-subspace distance query*, with approximation guarantees,
- an experimental evaluation showing that a year of history from thousands of sensors is possible to process in minutes to answer point-to-subspace distance queries in milliseconds.

2 A Model For Events

Our goal in this paper is to build a model of what is a non-event across many time-series, possibly with *non-uniform sampling* across the time series, *missing values*, and *measurement errors* present in the values. For example, one could consider applications in urban traffic management, where the number of vehicles passing over induction loops are measured, but often prove to be noisy, with the reliability of the induction loops and the related communication infrastructure limited. Subsequently, we aim at an on-line event detection mechanism, which would be able to decide whether multiple fragments of multiple incoming time-series

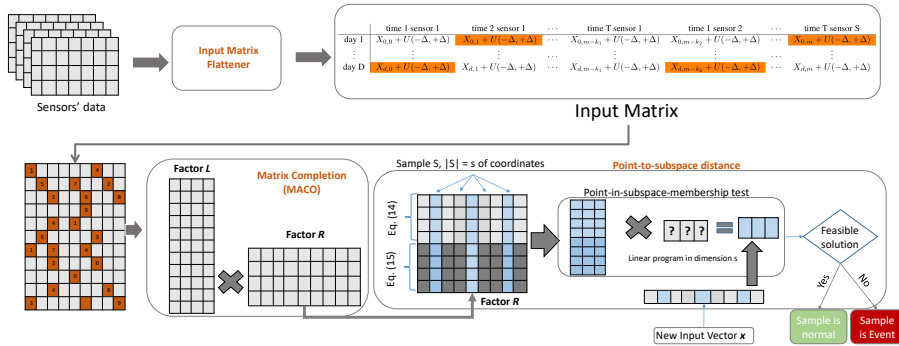


Figure 1: A schematic illustration of the model.

present an event (abnormal behaviour) or not. In urban traffic management, for example, one aims at detecting a road accident, based on the evolution of the traffic volumes across a network of induction loops. Notice that an accident will manifest itself by some readings being low, due to roads being blocked, while other readings being high, due to re-routing, while no induction loop has to have its readings more than a standard deviation away from the long-run average, which renders uni-variate methods difficult to use. Such monitoring problems are central to many Internet-of-Things applications.

Our model is based on the observation that there is a daily recurrent pattern in time series across many applications. Consider, for example, the volume of vehicles travelling over a road segment when computing the daily variation of demand for transportation, the current injected into a branch of a power system in the case of electric power, or the flow through a pipe in the case of a water system. These follow a bi-modal pattern with morning and evening peak. This pattern can be exploited by storing each day worth of data as a row in a matrix, possibly with many missing values. For multiple time-series, we obtain multiple partial matrices, or a partial tensor. These can be flattened by concatenating the matrices row-wise to obtain one large matrix, as suggested in Figure 1. For D days discretised to T periods each, with up to S sensors available, the flattened matrix M is in dimension $n = TS$ and has $m = D$ rows.

Considering this flattened representation, it is natural to assume that each new day looks like a linear combination of r prototypical days, or rows in the flattened matrix in dimension $m \gg r$. Formally, we assume that there exists $R \in \mathbb{R}^{r \times n}$, such that our observations $x \in \mathbb{R}^n$ are

$$x = cR + \mathcal{U}(-\Delta, \Delta), \quad (1)$$

possibly with many values missing, for some coefficients $c \in \mathbb{R}^r$ weighing the r vectors $\{e_1, e_2, \dots, e_r\}$ row-wise in R , with uniformly-distributed noise \mathcal{U} between $-\Delta$ and Δ .

We compute matrix R , using low-rank approximation of the flattened matrix with an explicit consideration of the uniformly-distributed error in the

measurements M_{ij} for $(i, j) \in M$. Considering the interval uncertainty set $[M_{ij} - \Delta, M_{ij} + \Delta]$ around each observation, this can be seen as matrix completion with element-wise lower bounds $X_{ij}^{\mathcal{L}} := M_{ij} - \Delta$ for $(i, j) \in M$ and element-wise upper bounds $X_{ij}^{\mathcal{U}} := M_{ij} + \Delta$ for $(i, j) \in M$. (Henceforth we use calligraphic \mathcal{L} for bounds from below and \mathcal{U} for bounds from above.) To formalise the factorisation $M \approx LR$, let $L_{i:}$ and $R_{:j}$ be the i -th row and j -th column of L and R , respectively. With Frobenius-norm regularisation, the completion problem we solve is:

$$\min_{L \in \mathbb{R}^{m \times r}, R \in \mathbb{R}^{r \times n}} f_{\mathcal{L}}(L, R) + f_{\mathcal{U}}(L, R) + \frac{\mu}{2} \|L\|_F^2 + \frac{\mu}{2} \|R\|_F^2 \quad (2)$$

where

$$f_{\mathcal{L}}(L, R) := \frac{1}{2} \sum_{(ij) \in \mathcal{L}} (X_{ij}^{\mathcal{L}} - L_{i:} R_{:j})_+^2, \quad (3)$$

$$f_{\mathcal{U}}(L, R) := \frac{1}{2} \sum_{(ij) \in \mathcal{U}} (L_{i:} R_{:j} - X_{ij}^{\mathcal{U}})_+^2, \quad (4)$$

where $\xi_+ = \max\{0, \xi\}$. Notice that this is a smooth, non-convex problem, whose special case of $\Delta = 0$ is NP-hard [29, 16].

Considering the factorization LR , where $L \in \mathbb{R}^{m \times r}$ and $R \in \mathbb{R}^{r \times n}$ obtained above (6), given an incoming $x \in \mathbb{R}^n$, the maximum likelihood estimate $\hat{c} \in \mathbb{R}^r$ of c in (1) is precisely the point minimizing $|x|_{\infty}$:

$$\min_{\hat{c} \in \mathbb{R}^r} \max_i |x_i - (\hat{c}R)_i| \quad (5)$$

whenever $\hat{c} \leq \Delta$. We refer to Section 7.1.1 of [5] for a discussion. In a linear program corresponding to (5), we consider a subset of coordinates of \mathbb{R}^n and prove a bound on the one-sided error when using the subset. This is the first use of a point-to-subspace query in ℓ^{∞} in event detection.

3 The Algorithms

In this section, we present the algorithms that we use with the above model. As outlined above, two algorithms are needed for the two problems. The first one is an *inequality-constrained matrix completion* algorithm, which estimates the low-rank approximation of the input matrix. In our experiments, this algorithm is run in an off-line fashion. The second algorithm is the *point-to-subspace proximity query*. As an input, it uses the output of the inequality-constrained matrix completion algorithm and it is able to predict if a new coming time series vector presents normal or abnormal behavior. The second algorithm is run in an on-line fashion. We describe the two algorithms in turn.

3.1 Matrix completion under interval uncertainty

The matrix completion under interval uncertainty can be seen as a special case of the inequality-constrained matrix completion of [25]:

$$\min\{f(L, R) : L \in \mathbb{R}^{m \times r}, R \in \mathbb{R}^{r \times n}\}, \quad (6)$$

Input: $\mathcal{E}, \mathcal{L}, \mathcal{U}, X^\mathcal{E}, X^\mathcal{L}, X^\mathcal{U}$, rank r

Output: $m \times n$ matrix

- 1: choose $L \in \mathbb{R}^{m \times r}$ and $R \in \mathbb{R}^{r \times n}$
- 2: **for** $k = 0, 1, 2, \dots$ **do**
- 3: choose random subset $\hat{S}_{\text{row}} \subset \{1, \dots, m\}$
- 4: **for** $i \in \hat{S}_{\text{row}}$ **in parallel do**
- 5: choose $\hat{r} \in \{1, \dots, r\}$ uniformly at random
- 6: compute $\delta_{i\hat{r}}$ using formula (11)
- 7: update $L_{i\hat{r}} \leftarrow L_{i\hat{r}} + \delta_{i\hat{r}}$
- 8: **end for**
- 9: choose random subset $\hat{S}_{\text{column}} \subset \{1, \dots, n\}$
- 10: **for** $j \in \hat{S}_{\text{column}}$ **in parallel do**
- 11: choose $\hat{r} \in \{1, \dots, r\}$ uniformly at random
- 12: compute $\delta_{\hat{r}j}$ using (12)
- 13: update $R_{\hat{r}j} \leftarrow R_{\hat{r}j} + \delta_{\hat{r}j}$
- 14: **end for**
- 15: **end for**
- 16: **return** LR

Algorithm 1: MACO: Matrix Completion via Alternating Parallel Coordinate Descent of [25]

where

$$f(L, R) := f_\mathcal{E}(L, R) + f_\mathcal{L}(L, R) + f_\mathcal{U}(L, R) + \frac{\mu}{2} \|L\|_F^2 + \frac{\mu}{2} \|R\|_F^2 \quad (7)$$

$$f_\mathcal{E}(L, R) := \frac{1}{2} \sum_{(i,j) \in \mathcal{E}} (L_{i:R:j} - X_{ij}^\mathcal{E})^2, \quad (8)$$

$$f_\mathcal{L}(L, R) := \frac{1}{2} \sum_{(i,j) \in \mathcal{L}} (X_{ij}^\mathcal{L} - L_{i:R:j})_+^2, \quad (9)$$

$$f_\mathcal{U}(L, R) := \frac{1}{2} \sum_{(i,j) \in \mathcal{U}} (L_{i:R:j} - X_{ij}^\mathcal{U})_+^2, \quad (10)$$

where for $(i, j) \in \mathcal{U}$ we have an element-wise upper bound $X_{ij}^\mathcal{U}$, for $(i, j) \in \mathcal{L}$ we have an element-wise lower bound $X_{ij}^\mathcal{L}$, for $(i, j) \in \mathcal{E}$ we know the exact value $X_{ij}^\mathcal{E}$, and $\xi_+ = \max\{0, \xi\}$.

A popular heuristic for matrix completion considers a product of two matrices, $X = LR$, where $L \in \mathbb{R}^{m \times r}$ and $R \in \mathbb{R}^{r \times n}$, obtaining $X = LR$ of rank at most r , cf. [35]. In particular, we use a variant of the alternating parallel coordinate descent method for matrix completion introduced by [25] under the name of ‘‘MACO’’, summarized in Algorithm 1. It is based on the observation that while f is not convex jointly in (L, R) , it is convex in L for fixed R and in R for fixed L . In Steps 3–8 of the algorithm, we fix R , choose random \hat{r} and a random set \hat{S}_{row} of rows of L , and update, in parallel, for $i \in \hat{S}_{\text{row}}$: $L_{i\hat{r}} \leftarrow L_{i\hat{r}} + \delta_{i\hat{r}}$. Following [25], we use

$$\delta_{i\hat{r}} := -\langle \nabla_L f(L, R), E_{i\hat{r}} \rangle / W_{i\hat{r}}, \quad (11)$$

Input: $L \in \mathbb{R}^{r \times n}$, $x \in \mathbb{R}^n$, $s, \Delta \in \mathbb{R}$
Output: true/false

- 1: choose $S \subset \{1, \dots, n\}$, $|S| = s$, uniformly at random
- 2: initialise a linear program P in variable $v \in \mathbb{R}^s$
- 3: **for** $i \in S$ **do**
- 4: add constraint $x_i - (\text{proj}_S(L)v)_i \leq \Delta$
- 5: add constraint $x_i - (\text{proj}_S(L)v)_i \geq -\Delta$
- 6: **end for**
- 7: **if** $\exists v \in \mathbb{R}^s$ such that the constraints are satisfied **then**
- 8: **return** true
- 9: **else**
- 10: **return** false
- 11: **end if**

Algorithm 2: Randomised point-in-subspace membership

where the computation of $\langle \nabla_L f(L, R), E_{\hat{r}_j} \rangle$ can be simplified considerably, as explained in [25]. In Steps 9–14, we fix L , choose random \hat{r} and a random set \hat{S}_{column} of columns of R , and update, in parallel for $j \in \hat{S}_{\text{column}}$: $R_{\hat{r}_j} \leftarrow R_{\hat{r}_j} + \delta_{\hat{r}_j}$.

$$\delta_{\hat{r}_j} := -\langle \nabla_R f(L, R), E_{\hat{r}_j} \rangle / V_{\hat{r}_j}, \quad (12)$$

where the computation of $\langle \nabla_R f(L, R), E_{\hat{r}_j} \rangle$ can, again, be simplified as suggested in Figure ??.

We should also like to comment on the choice of Δ and ϵ . A sensible approach seems to be based on cross-validation: out of the historical data (or out of L), one can pick one row, and compute the Δ needed. The maximum of Δ for any row seems to be a good choice. We refer to [25] for a discussion of the choice of the parameter $\mu > 0$.

3.2 Point-to-subspace queries in ℓ^∞

As suggested previously, instead of computing the distance of an incoming time-series to each one of those already available per-day time-series, classified as event or non-event, we consider a point-to-subspace query in the infinity norm:

$$\min_{\hat{c} \in \mathbb{R}^r} \max_i |x_i - (\hat{c}R)_i|, \quad (13)$$

and specifically the test whether the distance (13) is less than or equal to Δ . As we described in section 2 for uniform noise ℓ^∞ gives the maximum likelihood estimate. The infinity-norm is sometimes seen as difficult to work with, due of the lack of differentiability. However note, that it (13) can be recast as a test of feasibility of a linear programming problem:

$$\min_{\hat{c} \in \mathbb{R}^r} 1 \text{ s.t. } x_i - (\hat{c}R)_i \leq \Delta, \quad (14)$$

$$(\hat{c}R)_i - x_i \leq \Delta. \quad (15)$$

Alternatively, this is an intersection of hyperplanes, or a hyper-plane arrangement. As we will show in the following section, this geometric intuition is useful in the analysis of the algorithms.

In Algorithm 2 we present a test, which considers only a subset S , $|S| \ll n$ of coordinates, picked uniformly at random. As we show in the following section, this test has only a modest one-sided error.

4 An Analysis

Before we present the main result, let us remark on the convergence properties and run-time of both Algorithm 1 and Algorithm 2. Algorithm 1 has been proposed by [25]. They present a convergence result, which states that the method is monotonic and, with probability 1, $\lim_{k \rightarrow \infty} \inf \|\nabla_L f(L^{(k)}, R^{(k)})\| = 0$, and $\lim_{k \rightarrow \infty} \inf \|\nabla_R f(L^{(k)}, R^{(k)})\| = 0$. This applies in our case as well. One could provide a more refined analysis under some assumptions on the initialization [21].

Our main analytical result concerns the statistical performance of the point-to-subspace query. Informally, the randomized point-to-subspace distance query in Algorithm 2 has one-sided error: If the distance between the vector x and $\text{span}(R)$ is no more than Δ in ℓ^∞ , we never report otherwise. If however, the distance actually is more than Δ in ℓ^∞ , considering only a subset S of coordinates may ignore a coordinate where the distance is larger, and hence mis-report that the vector is within distance Δ in ℓ^∞ , with a certain probability, depending on the number of constraints that are actually violated. For example, to achieve the one-sided error of ϵ with probability of $1/3$ or less, this test needs to solve a linear program in dimension $O(\frac{r \log r}{\epsilon} \log \frac{r \log r}{\epsilon})$. Notice that this bound is independent of the “ambient” dimension n .

Formally:

Theorem 1. (i) When the distance (13) is $D \leq \Delta$, Algorithm 2 never reports the point is outside the sub-space. (ii) When the distance (13) is $D > \Delta$, because there are ϵn coordinates i such that for all \hat{c} , there is $|x_i - (\hat{c}R)_i| \geq \Delta$, then for any $\delta \in (0, 1)$, when Algorithm 2 considers s coordinates

$$O\left(\frac{1}{\epsilon} \log \frac{1}{\delta} + \frac{r \log r}{\epsilon} \log \frac{r \log r}{\epsilon}\right)$$

sampled independently uniformly at random, the point is inside the subspace with probability $1 - \delta$.

Proof. (Sketch) To see (i), consider the linear program constructed in Algorithm 2 and notice that its constraints are a subset of those in (14). If (14) is feasible, then any subset of constraints will be feasible. To see (ii), we use standard tools from computational geometry. In particular, we show that a certain set related to the polyhedron of feasible x , which is known as range space, has a small Vapnik-Chervonenkis (VC) dimension d . Subsequently, we apply the celebrated

result of [18], which states that for any range space of VC dimension d and $\epsilon, \delta \in (0, 1)$, if

$$O\left(\frac{1}{\epsilon} \log \frac{1}{\delta} + \frac{d}{\epsilon} \log \frac{d}{\epsilon}\right)$$

coordinates are sampled independently, we obtain an ϵ -net with probability at least $1 - \delta$. We refer to Appendix A for the details. \square

Next, let us consider the run-time of Algorithm 2, which is dominated by the feasibility test of a linear program P in Line 7. Using standard interior-point methods [14], if there is a feasible solution to the linear program P , an ϵ -accurate approximation to the can be obtained in $O(\sqrt{s} \ln(1/\epsilon))$ iterations, wherein a each iteration amounts to solving a linear system. This yields an upper bound on the run-time of

$$O\left(\frac{r^{3.5} \log^{3.5} r}{\epsilon^{3.5}} \log^{3.5} \frac{r}{\epsilon}\right),$$

which could be improved considerably, by exploiting the sparsity in the linear program’s constraint matrix. The same iterations make it possible to detect infeasibility using the arguments of [22], although the homogeneous self-dual approach of [42] with a somewhat worse iteration complexity may be preferable in practice. Either way, a solver-generator [27, 26] allows for excellent performance.

Alternatively, however, one may consider:

Theorem 2. *There is an algorithm that can pre-process a sample of s coordinates such that the point-in-subspace membership query can be answered in time $O(\log s)$ in the worst case. The expected run-time of the pre-processing is $O(s^{r+\epsilon})$, $\epsilon \geq 0$, where the expectation is with respect to the random behaviour of the algorithm, and remains valid for any input.*

Proof. (Sketch) Notice that one can replace the test of feasibility of a linear program P with a point-location problem in a hyperplane arrangement. We refer to [10, 34] for a very good introduction to hyperplane arrangements, but to provide an elementary intuition: An alternative geometric view of Algorithm 2 is that we have a subspace $P \subseteq \mathbb{R}^s$, initialise it to $P = \mathbb{R}^s$ in Line 2, and then intersect it with hyperplanes on Lines 4–5. Equally well, one may consider a hyper-plane arrangement P , initialise it to an empty set in Line 2, and then add hyperplanes on Lines 4–5. Our goal is not to optimise a linear function over P , but rather to decide whether there exists a point within P , the intersection of the hyperplanes, which corresponds to one cell of the arrangement. The actual result follows from the work of [8, 9] on hyperplane arrangements. \square

While we do not necessarily advocate the use of the algorithm of [9] in “pedestrian” applications, there may be large-scale use cases, where the asymptotics do matter and the sampling of the coordinates may be reused.

5 Experimental evaluation

In order to evaluate our approach, we have implemented both algorithms from scratch in Python, using Numpy [36] for numerical linear algebra and `multiprocess` for parallel processing.

The experiments were executed on a standard PC equipped with an Intel i7-7820X CPU and 64 GB of RAM.

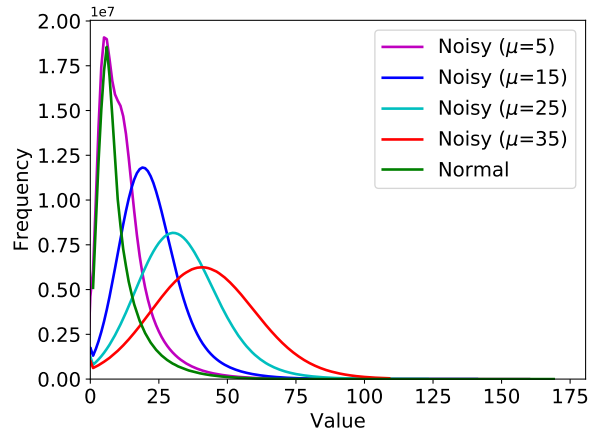
5.1 The Data

In our experiments, we have started with traffic-monitoring data collected at intersections in Dublin, Ireland, between January 1 and November 30, 2017. Therein, each time series is obtained by one induction loop at an approach to an intersection, with sensors at stop-lines and irregular intervals from stop-lines. Overall, our data contains readings from 3432 such sensors, distributed across the city.

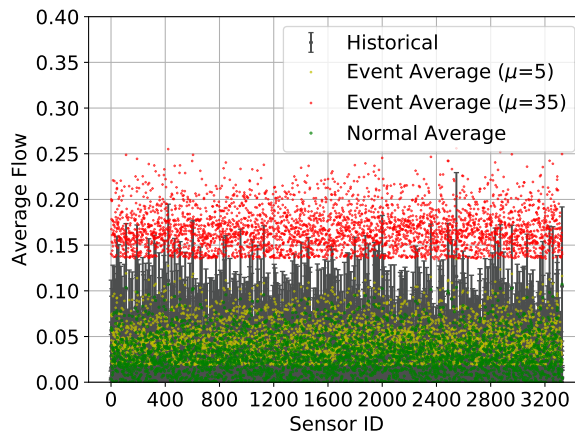
In order to use a realistic data set, reflecting the asynchronous operations of the system, we record the samples as they arrive asynchronously and do not impute any missing values. In particular, each intersection operates asynchronously, with all pre-defined phases changing, in turn, within a cycle time varying between 50 and 120 seconds both across the intersections and over time. Whenever an intersection’s cycle time finishes, we record the flow over the cycle time. Within any given time period, e.g., 2 minutes, we receive vehicle count data from only a fraction of the sensors. For each day, we consider data between 7 a.m. and 10 p.m., which are of particular interest to traffic operators.

5.2 The Results

As described above, the data for our experiments are from 3432 sensors distributed across Dublin, Ireland, as recorded between January and November 2017 at 2 minute intervals, if available. In the flattened matrix $X \in \mathbb{R}^{304,299430}$, there were 38767895 zeros out of the 91026720 elements, representing 42% sparsity. This is due to a large part to the asynchronicity of the sensor readings, and to a lesser part due to sensor failures. In order to evaluate our approach, we have created several matrices from X ; one similar to matrix X with a small amount of noise to represent normal behaviour and further matrices with more noise to represent events. Specifically, using rows of matrix X , we have created matrices Y and G in the following way. First, we have generated 1000 random scalars uniformly over $[0, 2]$ and we multiplied these scalars with rows sampled uniformly at random from matrix X (with repetition). This way, we have obtained 1200 new non-event time series, each of which was perturbed by independently identically uniformly distributed noise on $[-0.8\Delta, 0.8\Delta]$. This way, we obtain matrix $Y \in \mathbb{R}^{1200 \times 299430}$ representing normal behaviour. In order to validate the event detection, we have also added Gaussian noise to 200 rows of matrix Y sampled uniformly at random, with the mean $\mu = 5, 15, 25, 35$ of the Gaussian noise in four variants of $G \in \mathbb{R}^{200 \times 299430}$. Figure 1 illustrates the remainder of the process.



(a)

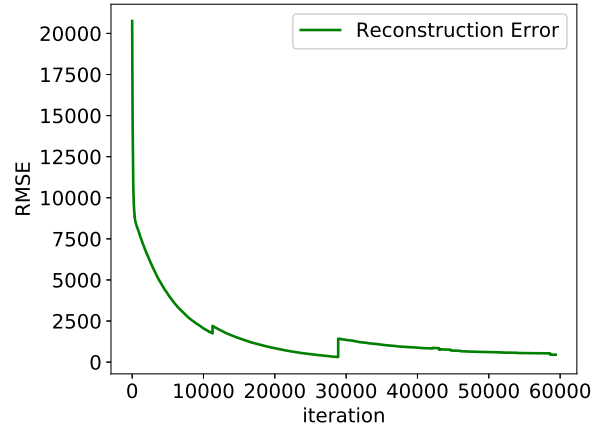


(b)

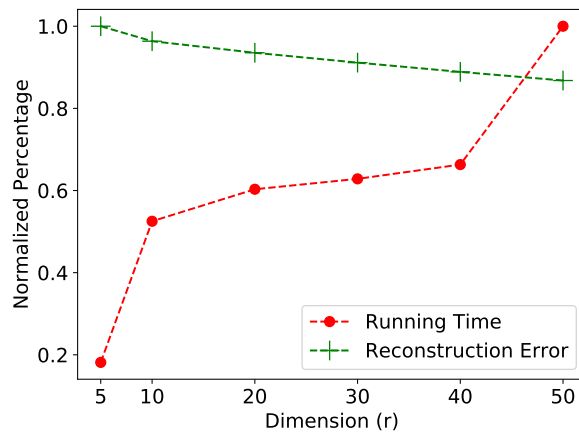
Figure 2: 2(b) The frequencies of the values reported from sensors, with and without additional Gaussian noise. 2(b) An illustration of the mean and standard deviation of the historical flow data at all available sensors (grey), plus the mean values for events (yellow for $\mu = 5$, red for $\mu = 35$) and non-events (green) at the same sensors.

We have trained our model using the first 1000 rows of matrix Y and we left the last 200 as ground truth for testing. We have evaluated our model using the last 200 entries of matrix Y and the 200 entries of matrix G with respect to recall, precision, and the so called F1 score, which is a harmonic mean of the former two measures.

Figure 3(b) presents a trade-off between time required for training and recon-



(a)



(b)

Figure 3: 3(a) A sample evolution of the reconstruction error (RMSE) over time for $r = 10$. 3(b) Training time until improvement in the error falls below 10^{-4} and reconstruction error, both plotted as a function of dimension r . Notice that the approach seems rather robust to the choice of r .

struction error in the choice of the dimension r . Notice that the reconstruction error is the usual extension of root mean square error to matrices, i.e., the Frobenius norm of the difference between matrix Y and LR . It is clear that increasing dimension value above 10 leads to marginal improvements in the reconstruction error, but increasing it above 40 leads to a sharp increase in training time. We chose $r = 10$ for our experiments. Figure 2(a) compares the readings of sensors from the non-event matrix Y with events in G , while omitting zeros. We can

observe that G with $\mu = 5$ is hard to distinguish from Y . Figure 2(b) presents the distribution of the values of the samples used for training: the average values of normal samples we used as input plotted in green and the average values of the samples of events (*i.e.*, sets with all Gaussian Noise mean values we used) plotted in red and yellow. We can observe that all supports of the distributions overlap, and especially in the case of $\mu = 5$ are very hard to distinguish.

In order to evaluate the performance of our subspace proximity tester, we have measured recall, precision and F1-score using different values of Δ on the 4 matrices G . Figures 4(a),4(b), 4(c) and 4 present the evolution of recall, precision and F1-score as a function of Δ for 4 different values of μ . We ran the experiment 5 times and present the mean. As can be observed, for small values of Δ , precision is high, while recall is low across all four G . This is the case, because small values of Δ lead to infeasibility of the LP. As we increase Δ , we observe that our approach identifies more of the input as *Normal*. On G matrices with $\mu = 15, 25, 35$, we can observe that values $\Delta > 20$ lead to the perfect performance with F1-Score of 1.0. We can also observe that for noise of a lesser magnitude ($\mu = 5$), the subspace proximity tester is able to identify samples from G with maximum F1-score of 0.7. By increasing Δ beyond this value, precision falls to 50%, which is due to the fact that too many input samples are classified as non-event. This behaviour is to be expected, because by increasing the value of Δ , we are “relaxing” the constraints of the linear program, which in turns leads to the non-event outcome being more common.

Finally, we note that in order to classify a new sample of dimensions $\mathbb{R}^{(1 \times 299430)}$, our subspace proximity tester requires approximately ~ 0.009 seconds for subset of cardinality $s = \log r \log(r/e)$ to obtain $e = 0.1$. We note that this does not use the algorithm of [9], and hence can be improved by many orders of magnitude, if needed.

6 Related work

Our particular method builds upon a rich history of research in low-rank matrix completion. There, [12] suggested to replace the rank with the nuclear norm in the objective. The corresponding use of semidefinite programming (SDP) has been very successful in theory [6], while augmented Lagrangian methods [19, 23, 31, 39] and alternating least squares (ALS) algorithms [33, 30] have been widely used in practice [33, 30, 28, 3, 15]. As it turns out [21, 20], they also allow for perfect recovery in some settings. Matrix completion has a number of applications in statistics, incl. functional data analysis [11]. The inequality-constrained variant of matrix completion, which we employ, has been introduced by [25]. The randomised subspace proximity testers are novel, as far as we can tell.

There is much related work in change-point and event detection. Since the work of Lorden [24], there has been much work on change-point detection in univariate time-series. See [2] for a book-length treatment. There are much fewer papers on the multi-variate problem [40, 1, 7, 43, 38] and fewer still, which

allow for the coping with missing data [40, 32]. From those, we differ in our assumptions (uniform noise) and the focus on efficient algorithms for the test.

In terms of the related work in urban traffic management, [41] propose a method for detecting traffic events that have impact on the road traffic conditions by extending the Bayesian Robust Principal Component Analysis. They create a sparse structure composed of multiple traffic data-streams (*e.g.*, traffic flow and road occupancy) and use it to localise traffic events in space and time. The data streams are subsequently processed so that with little computational cost they are able to detect events in an on-line and real-time fashion. [4] analyse road traffic accidents based on their severity using a space-time multivariate Bayesian model. They include both multivariate spatially structured and unstructured effects, as well a temporal component, to capture the dependencies between the severity and time effects, within a Bayesian hierarchical formulation.

7 Conclusions

We have presented a novel approach to event detection in high-dimensional data. The estimation of the normal subspace have been shown to scale to settings with tens of millions of observations across thousands of time series, while the event-or-not query allows for near-real-time response.

Due to the use of matrix-completion techniques in the training, as well the use of as a subset of coordinates in the point-to-subspace distance query, our approach is robust to missing values in the training data, and hence to sensor failures, clock failures, non-uniform sampling, and asynchronous operations, more generally. The particular matrix-completion algorithm we employ is robust to uniformly distributed noise, and the use of the particular point-to-subspace query is optimal when uniformly distributed noise is present, which makes the approach robust to measurement errors. Due to the non-parametric nature of the tester the approach, tuning is limited to the amount of measurement error expected and the rank of the low-rank approximation. In our experimental evaluation, we have tested the ability of the proposed algorithms to identify samples with abnormal behavior, even when the input samples were very hard to distinguish from normal data for a human person or simple approaches.

We envision this approach may have wide-ranging applications, wherever asynchronous high-dimensional data streams are present. Outside of traffic management, monitoring cloud computing facilities and electric power- and water-distribution networks, are prime examples.

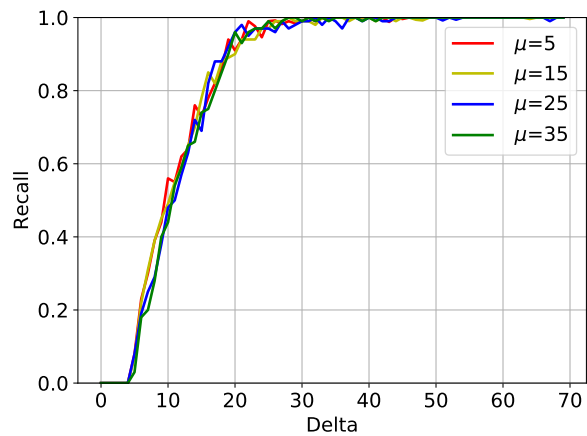
References

- [1] John AD Aston and Claudia Kirch. Change points in high dimensional settings. *arXiv preprint arXiv:1409.1771*, 2014.
- [2] Michèle Basseville, Igor V Nikiforov, et al. *Detection of abrupt changes: theory and application*, volume 104. Prentice Hall Englewood Cliffs, 1993.
- [3] R.M. Bell and Y. Koren. Scalable collaborative filtering with jointly derived neighborhood interpolation weights. In *IEEE 7th International Conference on Data Mining*, pages 43–52, Piscataway, NJ, USA, Oct 2007. IEEE.
- [4] Areti Boulieri, Silvia Liverani, Kees de Hoogh, and Marta Blangiardo. A spacetime multivariate bayesian model to analyse road traffic accidents by severity. *Journal of the Royal Statistical Society: Series A (Statistics in Society)*, 180(1):119–139, 2017.
- [5] Stephen Boyd and Lieven Vandenberghe. *Convex Optimization*. Cambridge University Press, New York, NY, USA, 2004.
- [6] Emmanuel J Candès and Benjamin Recht. Exact matrix completion via convex optimization. *Foundations of Computational Mathematics*, 9(6):717–772, 2009.
- [7] Haeran Cho and Piotr Fryzlewicz. Multiple-change-point detection for high dimensional time series via sparsified binary segmentation. *Journal of the Royal Statistical Society: Series B (Statistical Methodology)*, 77(2):475–507, 2015.
- [8] K L Clarkson. Further applications of random sampling to computational geometry. In *Proceedings of the Eighteenth Annual ACM Symposium on Theory of Computing*, STOC '86, pages 414–423, New York, NY, USA, 1986. ACM.
- [9] Kenneth L. Clarkson. New applications of random sampling in computational geometry. *Discrete & Computational Geometry*, 2(2):195–222, Jun 1987.
- [10] Mark De Berg, Marc Van Kreveld, Mark Overmars, and Otfried Cheong Schwarzkopf. *Computational geometry*. Springer, 2000.
- [11] Marie-Hélène Descary and Victor Michael Panaretos. Functional data analysis by matrix completion. *The Annals of Statistics*, page to appear, 2018.
- [12] Maryam Fazel. *Matrix Rank Minimization with Applications*. PhD thesis, Stanford University, 2002.
- [13] Bernd Gärtner and Michael Hoffmann. *Computational Geometry*. ETH, Zurich, CH, 2012. Draft dated January 15th, 2013.

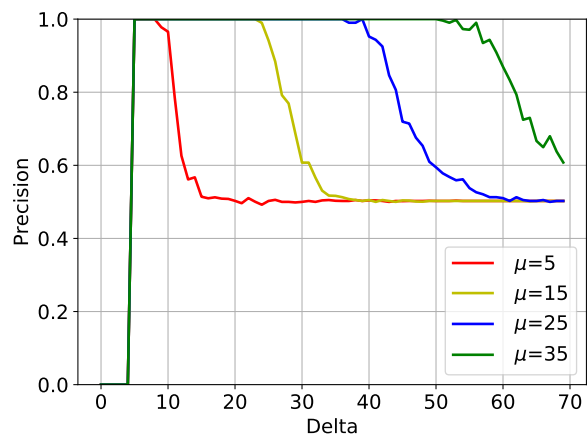
- [14] Jacek Gondzio. Interior point methods 25 years later. *European Journal of Operational Research*, 218(3):587 – 601, 2012.
- [15] J.P. Haldar and D. Hernando. Rank-constrained solutions to linear matrix equations using powerfactorization. *IEEE Signal Processing Letters*, 16(7):584–587, July 2009.
- [16] Nicholas JA Harvey, David R Karger, and Sergey Yekhanin. The complexity of matrix completion. In *Proceedings of the Seventeenth Annual ACM-SIAM Symposium on Discrete Algorithm*, pages 1103–1111, Philadelphia, PA, USA, 2006. Society for Industrial and Applied Mathematics.
- [17] D Haussler and E Welzl. Epsilon-nets and simplex range queries. In *Proceedings of the Second Annual Symposium on Computational Geometry*, SCG '86, pages 61–71, New York, NY, USA, 1986. ACM.
- [18] David Haussler and Emo Welzl. ϵ -nets and simplex range queries. *Discrete & Computational Geometry*, 2(2):127–151, Jun 1987.
- [19] Martin Jaggi and Marek Sulovský. A simple algorithm for nuclear norm regularized problems. In *Proceedings of the 27th International Conference on Machine Learning (ICML 10)*, pages 471–478, New York, NY, USA, 2010. ACM.
- [20] Prateek Jain, Praneeth Netrapalli, and Sujay Sanghavi. Low-rank matrix completion using alternating minimization. In *Proceedings of the forty-fifth annual ACM symposium on Theory of computing*, pages 665–674, New York, NY, USA, 2013.
- [21] Raghunandan H Keshavan, Andrea Montanari, and Sewoong Oh. Matrix completion from a few entries. *IEEE Transactions on Information Theory*, 56(6):2980–2998, 2010.
- [22] Masakazu Kojima, Nimrod Megiddo, and Shinji Mizuno. A general framework of continuation methods for complementarity problems. *Mathematics of Operations Research*, 18(4):945–963, 1993.
- [23] Kiryung Lee and Y. Bresler. Admira: Atomic decomposition for minimum rank approximation. *IEEE Transactions on Information Theory*, 56(9):4402–4416, Sept 2010.
- [24] Gary Lorden. Procedures for reacting to a change in distribution. *The Annals of Mathematical Statistics*, pages 1897–1908, 1971.
- [25] Jakub Mareček, Peter Richtárik, and Martin Takáč. Matrix completion under interval uncertainty. *European Journal of Operational Research*, 256(1):35–43, 2017.
- [26] Jacob Mattingley and Stephen Boyd. Cvxgen: A code generator for embedded convex optimization. *Optimization and Engineering*, 13(1):1–27, 2012.

- [27] John Mattingley and Stephen Boyd. Real-time convex optimization in signal processing. *IEEE Signal processing magazine*, 27(3):50–61, 2010.
- [28] Andriy Mnih and Ruslan Salakhutdinov. Probabilistic matrix factorization. In *Advances in Neural Information Processing Systems 20*, pages 1257–1264, Red Hook, NY, USA, 2007. Curran Associates, Inc.
- [29] Balas Kausik Natarajan. Sparse approximate solutions to linear systems. *SIAM Journal on Computing*, 24(2):227–234, 1995.
- [30] Jasson D. M. Rennie and Nathan Srebro. Fast maximum margin matrix factorization for collaborative prediction. In *Proceedings of the 31st International Conference on Machine Learning (ICML 14)*, pages 713–719, New York, NY, USA, 2005. ACM.
- [31] Shai Shalev-Shwartz, Alon Gonen, and Ohad Shamir. Large-scale convex minimization with a low-rank constraint. In *Proceedings of the 28th International Conference on Machine Learning (ICML 11)*, pages 329–336, New York, NY, USA, 2011. ACM.
- [32] Yong Sheng Soh and Venkat Chandrasekaran. High-dimensional change-point estimation: Combining filtering with convex optimization. *Applied and Computational Harmonic Analysis*, 43(1):122–147, 2017.
- [33] Nathan Srebro, Jason Rennie, and Tommi S Jaakkola. Maximum-margin matrix factorization. In *Advances in Neural Information Processing Systems 17 (NIPS 2004)*, pages 1329–1336, Red Hook, NY, USA, 2004. Curran Associates, Inc.
- [34] Richard P Stanley. *An Introduction to Hyperplane Arrangements*. IAS/Park City Mathematics Institute, Park City, Utah, USA, 2004.
- [35] Jared Tanner and Ke Wei. Normalized iterative hard thresholding for matrix completion. *SIAM Journal on Scientific Computing*, 35(5), 2013.
- [36] Stfan van der Walt, S. Chris Colbert, and Gaël Varoquaux. The numpy array: A structure for efficient numerical computation. *Computing in Science & Engineering*, 13(2):22–30, 2011.
- [37] VN Vapnik and A Ya Chervonenkis. On the uniform convergence of relative frequencies of events to their probabilities. *Theory of Probability and its Applications*, 16(2):264, 1971.
- [38] G. Wang, C. Zou, and G Yin. Change-point detection in multinomial data with a large number of categories. *The Annals of Statistics*, page to appear, 2018.
- [39] Zheng Wang, Ming-Jun Lai, Zhaosong Lu, Wei Fan, Hasan Davulcu, and Jieping Ye. Rank-one matrix pursuit for matrix completion. In *Proceedings of the 31st International Conference on Machine Learning (ICML 14)*, pages 91–99, New York, NY, USA, 2014. ACM.

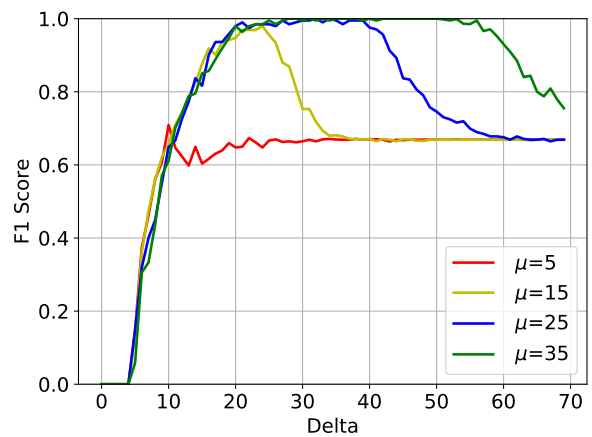
- [40] Yao Xie, Jiaji Huang, and Rebecca Willett. Change-point detection for high-dimensional time series with missing data. *IEEE Journal of Selected Topics in Signal Processing*, 7(1):12–27, 2013.
- [41] S. Yang, K. Kalpakis, and A. Biem. Detecting road traffic events by coupling multiple timeseries with a nonparametric bayesian method. *IEEE Transactions on Intelligent Transportation Systems*, 15(5):1936–1946, Oct 2014.
- [42] Yinyu Ye, Michael J. Todd, and Shinji Mizuno. An $o(\sqrt{nl})$ -iteration homogeneous and self-dual linear programming algorithm. *Mathematics of Operations Research*, 19(1):53–67, 1994.
- [43] Changliang Zou, Zhaojun Wang, Xuemin Zi, and Wei Jiang. An efficient online monitoring method for high-dimensional data streams. *Technometrics*, 57(3):374–387, 2015.



(a) Recall



(b) Precision



(c) F1-Score

Figure 4: Recall, precision and F1-score as a function of Δ . For noise of large-enough magnitude ($\mu = 25, \mu = 35$), one can obtain F1 score of 1 for a modest range of Δ .

A Proof of the Main Theorem

As suggested earlier, our goal is to prove Theorem 1, which we restate here for convenience:

Theorem. (i) When the distance (13) is $D \leq \Delta$, Algorithm 2 never reports the point is outside the sub-space. (ii) When the distance (13) is $D > \Delta$, because there are ϵn coordinates i such that for all \hat{c} , there is $|x_i - (\hat{c}R)_i| \geq \Delta$, then for any $\delta \in (0, 1)$, when Algorithm 2 considers s coordinates

$$O\left(\frac{1}{\epsilon} \log \frac{1}{\delta} + \frac{r \log r}{\epsilon} \log \frac{r \log r}{\epsilon}\right)$$

sampled independently uniformly at random, the point is inside the subspace with probability $1 - \delta$.

To see (i), consider the linear program constructed in Algorithm 2 and notice that its constraints are a subset of those in (14). If (14) is feasible, then any subset of constraints will be feasible.

To see (ii), we show that a set related to the polyhedron of feasible x has a small Vapnik-Chervonenkis (VC) dimension and apply classical results from discrete geometry. In particular, we proceed in four steps:

1. denote by \mathcal{S}_1 the range space for all possible constraints added in Line 4 and by \mathcal{S}_2 the range space for all possible constraints added in Line 5.
2. The VC dimension of each of $\mathcal{S}_1, \mathcal{S}_2$ is at most $r + 1$.
3. The VC dimension of $\mathcal{S}_1 \cup \mathcal{S}_2$ is $O(r \log r)$.
4. Subsequently, we apply the celebrated result:

Theorem 3 ([17, 18, 8, 9]). *Let $(\mathcal{X}, \mathcal{R})$ be a range space of Vapnik-Chervonenkis dimension d . Let $\epsilon, \delta \in (0, 1)$. If \mathcal{S} is a set of*

$$O\left(\frac{1}{\epsilon} \log \frac{1}{\delta} + \frac{d}{\epsilon} \log \frac{d}{\epsilon}\right)$$

points sampled independently from a finite subset of \mathcal{X} , then \mathcal{S} is an ϵ -net for the finite subset with probability at least $1 - \delta$.

To develop these ideas formally, let us reiterate the usual definitions of discrete geometry using the notation of [37] and [18], which partly overlaps with the notation used in the paper. We use calligraphic fonts in this appendix to distinguish \mathcal{S} of the main body of the paper from \mathcal{S} of the appendix, etc.

Definition 4 (Range space of [37]). *A range space \mathcal{S} is a pair $(\mathcal{X}, \mathcal{R})$, where \mathcal{X} is a set and \mathcal{R} is a family of subsets of \mathcal{X} , $\mathcal{R} \subseteq 2^{\mathcal{X}}$. Members of \mathcal{X} are called elements or points of \mathcal{S} and members of \mathcal{R} are called ranges of \mathcal{S} . \mathcal{S} is finite if \mathcal{X} is finite.*

Notice that the range space is a (possibly infinite) hypergraph.

Definition 5 (Shattering of [37]). *Let $\mathcal{S} = (\mathcal{X}, \mathcal{R})$ be a range space and let $\mathcal{A} \subset \mathcal{X}$ be a finite set. Then $\Pi_{\mathcal{R}}(\mathcal{A})$ denotes the set of all subsets of \mathcal{A} that can be obtained by intersecting \mathcal{A} with a range of \mathcal{S} . If $\Pi_{\mathcal{R}}(\mathcal{A}) = 2^{\mathcal{A}}$, we say that \mathcal{A} is shattered by \mathcal{R} .*

Definition 6 (Dimension of [37]). *The Vapnik-Chervonenkis dimension of \mathcal{S} is the smallest integer d such that no $\mathcal{A} \subset \mathcal{X}$ of cardinality $d + 1$ is shattered by \mathcal{R} . If no such d exists, we say the dimension of \mathcal{S} is infinite.*

Definition 7 (ϵ -net of [17]). *An ϵ -net of a finite subset of points $P \subseteq \mathcal{X}$ is a subset $\mathcal{N} \subseteq P$ such that any range $\nabla \in \mathcal{R}$ with $|\nabla \cap P| \geq \epsilon|P|$ has a non-empty intersection with \mathcal{N} .*

Step 1. The range spaces \mathcal{S}_1 and \mathcal{S}_2 will share the same set of points, namely $[n] := 1, 2, \dots, n$, and feature very similar ranges: \mathcal{S}_1 will feature the hyperplanes $x_i - (\hat{c}R)_i \leq \Delta$ corresponding to the first set of constraints in the LP (14), while \mathcal{S}_2 will feature the hyperplanes $(\hat{c}R)_i - x_i \leq \Delta$. We keep them separate, so as to allow for the hyperplanes to be in a generic position.

Alternatively, one could construct a single range space, with the same set of points and ranges given by the subspaces given by the intersections of $x_i - (\hat{c}R)_i \leq \Delta$ and $(\hat{c}R)_i - x_i \leq \Delta$ for $i \in [n]$. This would, however, complicate the analysis, somewhat.

Step 2. The VC dimension of each of $\mathcal{S}_1, \mathcal{S}_2$ is at most $r + 1$. For range spaces, where the ranges are hyper-planes, this is a standard result. We refer to Section 15.5.1 of [13] for a very elegant proof using Radon's theorem. Notice that r would suffice, if there were no vertical hyperplanes.

Step 3. The VC dimension of $\mathcal{S}_1 \cup \mathcal{S}_2$ is $O(r \log r)$. This follows by the counting of the possible ranges and Sauer-Shelah lemma, a standard result. We refer to Lemma 15.6 in [13].

Step 4. The intuition is that if there is a large-enough subset, a large-enough random sample will intersect with it. The surprising part of Theorem 3 on the existence of ϵ -nets is that the bound of the large-enough does not depend on the number of points of the ground set, but only on the VC dimension established above. In particular, we sample coordinates $S, |S| = s$ in Line 1. This corresponds to sampling from \mathcal{X} in $\mathcal{S}_1 \cup \mathcal{S}_2$. Because we assume there are ϵn coordinates i such that such that for all \hat{c} , there is $|x_i - (\hat{c}R)_i| \geq \Delta$, an ϵ -net will intersect these by Theorem 3.